Optical fiber coupling to planar photonic crystal microcavities

Paul E. Barclay,* Kartik Srinivasan, and Oskar Painter

Department of Applied Physics, California Institute of Technology, Pasadena, California 91125
(Dated: February 2, 2008)

A technique is demonstrated which efficiently transfers light between a tapered standard single-mode optical fiber and a resonant mode of a high-Q photonic crystal cavity with mode volume less than a cubic wavelength in size. Cavity mode quality factors of 4.7×10^4 are measured, and a total fiber-to-cavity coupling efficiency of 44% is demonstrated.

PACS numbers:

Recently it has been demonstrated that resonant microcavities formed in planar photonic crystals (PC) are capable of not only confining light to ultra-small optical mode volumes[1], but can also be made of high enough quality to enable photon cavity lifetimes capable of, for instance, reaching strong-coupling with atomic Cs[2] or semiconductor quantum dots[1, 3, 4]. In many of the proposed applications of such PC cavities in quantum, nonlinear, and integrated optics, the ability to efficiently interface the PC cavities with external optics is also of critical importance. In particular, using high-Q PC cavities for chip based cavity-QED (cQED) [2] or in single-photon sources [5], where photon collection is an important measure of device performance [6], requires an efficient coupling scheme to the sub-micron cavity mode. The difficulty in optically accessing PC cavities is largely a result of their ultra-small mode volumes and external radiation pattern, which unlike micropost [7] and Fabry-Perot [8] cavities, is not inherently suited to coupling with conventional free-space or fiber optics. In this Letter we present an optical fiber-based coupling technique, and employ it to efficiently source and collect light from the resonant modes of a high-Q PC cavity.

An illustration of the coupling scheme is shown in Fig. 1(a). Evanescent coupling between an optical fiber taper [9] and a planar photonic crystal waveguide (PCWG) is initially used to interface with the PC chip. Once on the chip, light is guided to a PC cavity at the terminus of the PCWG. This PC cavity-waveguide system was previously studied in Refs. [10], where the fundamental (TE_1) mode of the PCWG (Fig. 1(c)) was designed to mode-match with the fundamental (A_2) cavity mode (Fig. 1(b)). The mode-matched cavity acts as a mirror with high reflectivity, $r_o(\omega)$, except at the frequencies of the localized cavity states, where light can resonantly tunnel between the PCWG and the cavity. The reflected signal from the PC cavity is finally recollected into the backward propagating fiber taper mode. Previous measurements of the optical fiber-PCWG evanescent coupler have shown that near unity coupling efficiency (97%) over a bandwidth of roughly 15 nm[11] is possible, and in an independent study, the A_2 mode of the graded square lattice PC cavity was measured to have a Q-factor of 4×10^4 and a mode localization consistent with an effective mode volume of
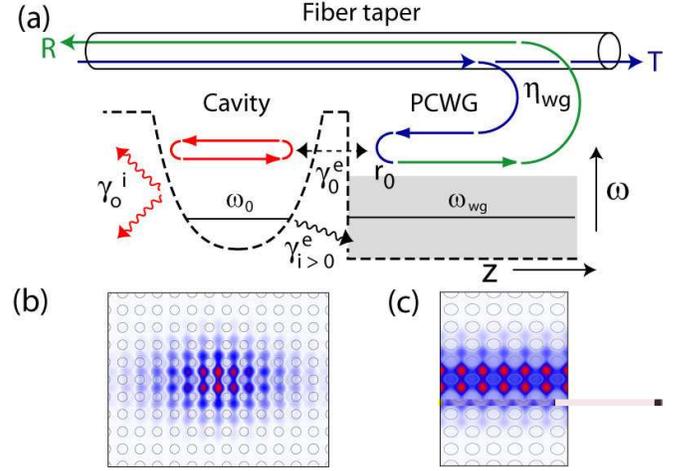

FIG. 1: (a) Illustration of the fiber-PC cavity coupling process. The dashed line is meant to represent the band-edge frequency in the planar PC as a function of the position z along the waveguide axis, with the shaded region representing the bandwidth of the fundamental PCWG mode. Magnetic field profile of (b) the high-Q PC cavity A_2 mode, and (c) the fundamental TE_1 PCWG mode.

$V_{\rm eff} = 0.9(\lambda/n)^3$[1]. In this work we aim to study the efficiency with which the PCWG can load the PC cavity using this fiber-coupled approach.

As proposed in Ref. [12], the interaction between the PC cavity and the external PCWG can be described by two key parameters, the *coupling parameter* K and the *ideality factor* I:

$$K \equiv \frac{\gamma_0^e}{\gamma_o^i + \sum_{i \neq 0} \gamma_i^e}, \tag{1}$$

$$I \equiv \frac{\gamma_0^e}{\sum_i \gamma_i^e}, \tag{2}$$

where the cavity mode is characterized by its resonance frequency ω_o, its intrinsic photon loss rate (γ_o^i) in absence of the external PCWG, and its coupling rates to the fundamental (TE_1 mode) and higher order (including radiating) modes of the external PCWG, γ_0^e and $\gamma_{i>0}^e$, respectively. I and K describe the degree of "good" loading (via the PCWG TE_1 mode in this case) rela-
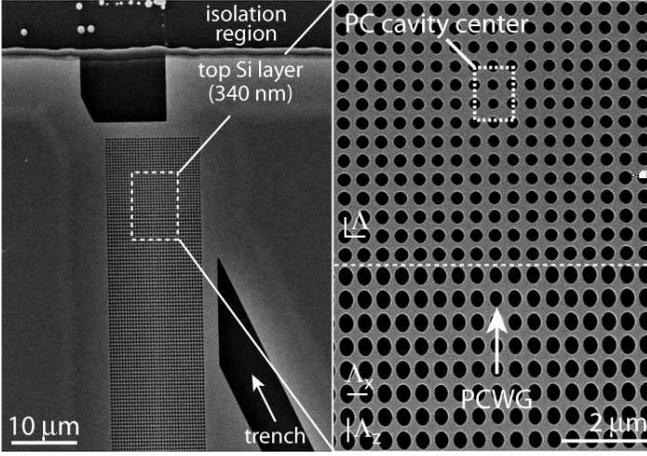
FIG. 2: SEM image of an integrated PCWG-PC cavity sample. The PC cavity and PCWG have lattice constants $\Lambda \sim 430$ nm, $\Lambda_x \sim 430$ nm, and $\Lambda_z \sim 550$ nm. The surrounding silicon material has been removed to form a diagonal trench and isolated mesa structure to enable fiber taper probing.

tive to the total loading of the resonator, and the parasitic and intrinsic loss channels of the resonator, respectively. On resonance, the fraction of the optical power reflected by the cavity back into the PCWG mode is given by, $R_o(\omega_o) = (1 - K)^2/(1 + K)^2$. The remaining (fractional) optical power, $1 - R_o(\omega_o)$, is absorbed inside the PC cavity or radiated into the parasitic output channels. The measured reflection resonance linewidth is given by the sum of the loss rates for *all* of the loss channels, $\delta\omega = \gamma_o^i + \sum_i \gamma_i^e$. The quality factor of the PC cavity mode due to intrinsic and parasitic loss (i.e., those loss channels other than the "good" PCWG TE_1 channel) can then be determined from $R_o(\omega_o)$ and $\delta\omega$,

$$Q_{i+P} = 2Q_T \frac{1}{1 \pm \sqrt{R_o(\omega_o)}} = Q_T(1 + K), \qquad (3)$$

where the total loaded quality factor is $Q_T = \omega_o/\delta\omega$, and where the $\pm$ corresponds to under- and over- coupled ($K \lessgtr 1$), respectively. On resonance, full power transfer (critical coupling) from the "good" loading channel to the resonant PC cavity mode occurs when $K = 1$.

Whereas K determines the amount of power dropped by the resonator, the role of I is more subtle. In the case of an internal emitter, the collection efficiency (η_0) of emitted photons into the "good" loading channel is,

$$\eta_0 = \frac{\gamma_0^e}{\gamma_o^i + \sum_i \gamma_i^e} = \frac{1}{1 + 1/K}. \qquad (4)$$

The quality factor of the loaded resonant cavity mode can be written in terms of K, I, and Q_i as $Q_T/Q_i = 1 - K/(I(1 + K)) = 1 - \eta_0/I$. Thus, for a given collection efficiency, to maximize the photon lifetime in the cavity I should be maximized. For non-linear optical phenomena, where the peak electric-field strength

inside the resonant cavity is an important parameter, one can write for the on-resonance internal stored energy $U = (1 - R_o(\omega_o))Q_{i+P}P_i$, where P_i is the input power in the "good" loading channel. The maximum stored energy in the resonator occurs at $K_{\max} = I/(2 - I)$, giving a peak stored energy $U_{\max} = I(Q_i/\omega_o)P_i$ which scales directly with I.

The integrated PC cavity-waveguide design employed here has two important features which serve to maximize I: (i) the waveguide and cavity modes have similar transverse field profiles (see Figs. 1(b-c)) which allows the cavity to be efficiently loaded end-on, and (ii) the end-fire PCWG-cavity geometry restricts the cavity to a single dominant output channel, in contrast to side-coupled geometries [4] in which the cavity radiates equally into backward and forward propagating PCWG modes (bounding $K < 1$ and $I \leq 0.5$). The geometry in this PC cavity-waveguide system is analogous to a Fabry-Perot cavity with a high reflectivity back mirror and a lower reflectivity front mirror through which a mode-matched input beam sources the cavity.

In this work, the PC cavity and PCWG devices were fabricated in an optically thin layer (thickness 340 nm) of silicon as described in Ref. [13]. As shown in Fig. 3, a trench extending diagonally from the cavity was defined to allow direct cavity probing[1]. Also, for these devices the loading of the PC cavity was set by the 9 periods of air holes between the center of the PC cavity and the end of the PCWG. A fiber-coupled swept wavelength (1565 - 1625 nm) laser source was used to measure the wavelength dependent forward transmission ($\bar{T}$) through the fiber taper. The reflected signal in the backward propagating fiber taper mode ($\bar{R}$) was also monitored in order to study the reflective properties of the PC cavity.

With the fiber taper placed above and parallel the PCWG, at phase-matching $\bar{T}$ decreases resonantly as power is coupled from the taper into the PCWG. Coupling to the TE_1 PCWG mode was verified by studying its dispersive and spatial properties[13]. The frequency of the A_2 cavity mode was also independently determined by probing the cavities directly with the fiber taper as described in Ref. [1]. Two mechanisms were then employed to bring the fiber taper-PCWG coupling bandwidth into resonance with an A_2 cavity mode. Coarse tuning was obtained by adjusting, from sample to sample, the nominal hole size and longitudinal lattice constant (Λ_z) of the PCWG. Fine tuning of the coupler's center wavelength over a 100 nm wavelength range was obtained by adjusting the position, and hence diameter, of the fiber taper region coupled to the PCWG.

Figure 3(a) shows the normalized reflected fiber signal, $\bar{R}$, for a taper diameter $d \sim 1$ μm which aligns the taper-PCWG coupler bandwidth with that of the A_2 PC cavity mode. This signal is normalized to the taper transmission in absence of the PCWG, and since light passes through the taper-PCWG coupler twice, is
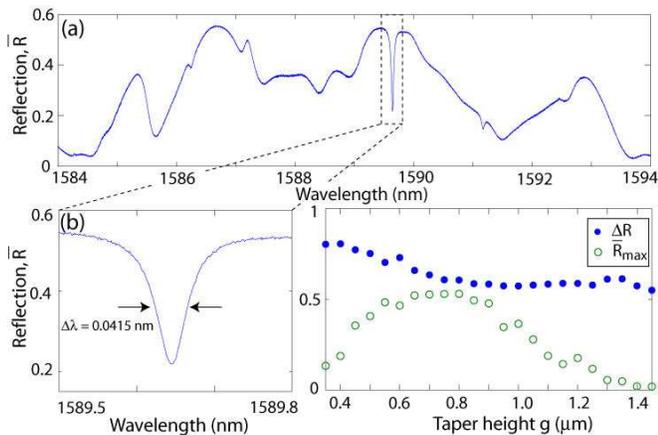
FIG. 3: (a) Measured reflected taper signal as a function of input wavelength (taper diameter $d \sim 1~\mu$m, taper height $g = 0.80~\mu$m). The sharp dip at $\lambda \sim 1589.7$ nm, highlighted in panel (b), corresponds to coupling to the A_2 cavity mode. (c) Maximum reflected signal (slightly detuned from the A_2 resonance line), and resonance reflection contrast as a function of taper height.

given by $\bar{R} = \eta_{wg}^2 R_o$ (note that both R_o and η_{wg} are frequency dependent). In Figure 3(a), the peak in $\bar{R}$ around $\lambda \sim 1590$ nm corresponds to the phase-matched point of the fiber taper and the TE_1 PCWG mode. From the peak value of $\bar{R}_{\max} = 0.53$, a peak taper-PCWG coupling efficiency of $\eta_{wg} \sim 73\%$ is estimated (where the off-resonant R_o is assumed to be unity). This value is lower than the 97% obtained in previous work[11] due to coupling to additional higher-order (normal to the Si slab) PCWG modes which interfere with the coupling to the fundamental TE_1 PCWG mode for strong taper-PCWG coupling. This can be avoided in future devices by increasing the nominal PCWG hole size relative to that in the PC-cavity or reducing the Si slab thickness, effectively freezing out the higher-order PCWG modes[13].

The sharp dip in reflection at $\lambda \sim 1589.7$ nm, shown in detail in Fig. 3(b), corresponds to resonant excitation of the A_2 PC cavity mode, as confirmed by direct fiber probing of the cavity. The other broad features in $\bar{R}$ correspond to weak Fabry-Perot effects of the PCWG. The reflected fiber taper signal as a function of taper-PCWG hap height, g, is shown in Fig. 3(c). For $g \geq 0.8~\mu$m, $\bar{R}_{\max}$ increases with decreasing g as the coupling from the fiber taper to the TE_1 PCWG mode becomes stronger. The reflection contrast, $\Delta R = 1 - R_o(\omega_o) = (\bar{R}_{\max} - \bar{R}(\omega_o))/\bar{R}_{\max}$, however, remains constant since the PCWG-cavity interaction is independent of the fiber taper to PCWG coupling. For smaller taper-PCWG gap heights, $g < 0.8~\mu$m, fiber taper coupling into higher order PCWG modes and radiation modes becomes appreciable, and $\bar{R}_{\max}$ decreases for decreased taper height. The corresponding increase in

ΔR seen in Fig. 3(c) is a result of interference between the TE_1 mode and higher-order PCWG modes which are excited and collected by the taper, and is not a manifestation of improved coupling between the TE_1 PCWG mode and the A_2 PC cavity mode.

From a Lorentzian fit to the A_2 cavity resonance dip, the normalized on-resonance reflected power is estimated to be $R_o(\omega_o) = 0.40$, corresponding to an undercoupled $K = 0.225$, with a loaded quality factor of $Q_T = 3.8 \times 10^4$. Substituting these values into Eq. (3) gives for the cavity mode quality factor due to parasitic loading and intrinsic losses, $Q_{i+P} = 4.7 \times 10^4$. Previous measurements of similar PC cavity devices without an external PCWG load yielded intrinsic quality factors of 4×10^4 [1], strongly indicating that the parasitic loading of the PC cavity by the PCWG is minimal, and $I \sim 1$ for this PC cavity-waveguide system. The input power dependence of the lineshape of the A_2 PC cavity mode was also investigated, with thermal bistability observed for input powers as small as 1 mW. Further details of these measurements will be reported elsewhere.

The efficiency of power transfer from the fiber taper into the PC cavity is given by, $\eta_{in} = \eta_{wg}\Delta R \approx 44\%$, which corresponds to the *total* percentage of photons input to the fiber taper which are dropped by the PC-cavity (the fiber taper itself typically has a loss of less than 10%). In the case of an internal emitter light source, the efficiency of collection into the fiber taper for this PC cavity system would be, $\eta_{out} = \eta_{wg}\eta_0 \approx 13\%$ ($\eta_0 \approx 18\%$). Previous measurements of near-ideal coupling between the fiber taper and PCWG[11] indicate that by adjusting the PCWG as described above, η_{in} and η_{out} can be increased to 58% and 18%, respectively. More substantially, adjustements in the coupling parameter K towards over-coupling by decreasing the number of air-hole periods between the PC cavity and the PCWG can result in significant increases in η_{in} and η_{out} with minimal penalty in loaded Q-factor for $I \sim 1$.

In conclusion, we have demonstrated an optical fiber coupling scheme to efficiently source and collect light from high-Q ultra-small mode volume PC cavities. This technique should be useful for future experiments in nonlinear optics and cQED, where efficient optical interfacing to planar PC cavities is important.

---

* Electronic address: pbarclay@caltech.edu
[1] K. Srinivasan, P. E. Barclay, M. Borselli, and O. Painter, Submitted to PRL, available online at http://arXiv.org/quant-ph/0309190 (2003).
[2] B. Lev, K. Srinivasan, P. E. Barclay, O. Painter, and H. Mabuchi, http://arxiv.org/abs/quant-ph/0402093, to appear in Nanotechnology (2004).
[3] K. Srinivasan, P. E. Barclay, O. Painter, J. Chen, A. X. Cho, and C. Gmachl, Appl. Phys. Lett. **83**(10), 1915

(2003).

[4] Y. Akahane, T. Asano, B.-S. Song, and S. Noda, Nature **425**, 944 (2003).

[5] J.-M. Gerard, *Solid State Cavity-Quantum Electrodynamics with Self-Assembled Quantum Dots* (Springer-Verlag, Germany, 2003), pp. 269–314.

[6] G. Brassard, N. Lutkenhaus, T. Mor, and B. Sanders, Phys. Rev. Lett. **85**(6), 1330 (2000).

[7] M. Pelton, C. Santori, J. Vuckovic, B. Zhang, G. Solomon, J. Plant, and Y. Yamamoto, Phys. Rev. Lett. **89**, 299602 (2002).

[8] J. McKeever, A. Boca, A. D. Boozer, R. Miller, J. R. Buck, A. Kuzmich, and H. J. Kimble, Science **303**(5666),

1992 (2004).

[9] J. Knight, G. Cheung, F. Jacques, and T. Birks, Opt. Lett. **22**(15), 1129 (1997).

[10] P. E. Barclay, K. Srinivasan, and O. Painter, J. Opt. Soc. Am. B **20**(11), 2274 (2003).

[11] P. E. Barclay, K. Srinivasan, M. Borselli, and O. Painter, Opt. Lett. **29**(7), 697 (2004).

[12] S. M. Spillane, T. J. Kippenberg, O. J. Painter, and K. J. Vahala, Phys. Rev. Lett. **91**(4), 043902 (2003).

[13] P. E. Barclay, K. Srinivasan, M. Borselli, and O. Painter, To appear in Appl. Phys. Lett., available online at http://arXiv.org/quant-ph/0308070 (2003).